Journal of Thermal Analysis, Vol. 32 (1987) 281–292

COMPARATIVE THERMOGRAVIMETRIC STUDY OF CHLORINATIONS OF HEMATITE AND WUSTITE

I. Bertóti, I. S. Pap, T. Székely and *I. Z. Babievskaya**

RESERACH LABORATORY FOR INORGANIC CHEMISTRY
OF THE HUNGARIAN ACADEMY OF SCIENCES, P.O.B. 112, PF. 132,
H-1502 BUDAPEST, HUNGARY
*N.S. KURNAKOV'S INSTITUTE OF GENERAL AND INORGANIC CHEMISTRY,
ACADEMY OF SCIENCES OF THE USSR, MOSCOW, U.S.S.R.

(Received March 17, 1986)

The reactions of hematite and wustite with Cl_2, $COCl_2$, $CO+Cl_2$ and gaseous CCl_4 were studied by thermogravimetry, X-ray diffraction and computer-assisted thermodynamic calculations. During the chlorination of hematite, only gaseous products were formed. The apparent activation energies were calculated from the isothermal TG curves. The chlorination of wustite involves the formation and transformation of a series of solid chloride products. $FeCl_2$(s), $FeCl_3$(s) and FeOCl(s) were found as intermediates during chlorination with Cl_2 or Cl_2+CO, while only $FeCl_2$(s) was detected in reactions with $COCl_2$ oe CCl_4. The chlorinations of the iron oxides with various agents were compared, and the differences in reactivity sequences were established.

Chlorination is a useful tool for the processing of low-grade ores and can also be used for the removal of iron from raw materials. Because of its technical importance, the chlorination behaviour of hematite was investigated in some recent publications [1–5], but much less attention has been paid to the lower oxides of iron [1, 2].

Results on the thermodynamic calculations and kinetic investigations of the reactions of various iron oxides with Cl_2 [6], CCl_4 [7], $COCl_2$ and $CO+Cl_2$ [8] were published earlier. The present work involves a comparative TG study of the reactions of Fe_2O_3 and FeO with various agents (Cl_2, $CO+Cl_2$, $COCl_2$, CCl_4) in the temperature range 300–1200 K.

John Wiley & Sons, Limited, Chichester
Akadémiai Kiadó, Budapest

Experimental

TG measurements were carried out in a special reactor attached to a Mettler semimicro recording balance, as described earlier [9]. Ferric oxide of analytical grade (Reanal, $s^0 = 10$ m^2 g^{-1}) was used. Wustite samples were prepared from iron oxalate by thermal decomposition in N_2 ($s^0 = 0.4$ m^2 g^{-1}). The crystalline structure of the samples was checked by X-ray diffraction analysis.

The chlorinating agents used were phosgene of 3N, chlorine of 3N and carbon monoxide of 3N purity, and reagent grade CCl_4, which was introduced from a bubbler. Nitrogen of 4N purity, dried in the usual manner, was used as inert diluting gas.

Results and discussion

Thermodynamic calculations

Some equilibrium diagrams relating to the chlorination reactions are given in the literature [1, 10], but further thermodynamic calculations proved useful for evaluation of the equilibrium distribution of a large number of species in the systems studied. The equilibrium compositions of the gas and solid phases were determined with a computer-assisted free enthalpy minimization program in a wide temperature range at 10^5 Pa total pressure. The results on the $FeO + COCl_2$ system are shown in Figs 1 and 2. The equilibrium compositions of the solid and gaseous products are strongly dependent on the ratio of FeO to $COCl_2$. When iron oxide is in excess (Fig. 1, molar ratio 5 : 1), CO_2 is the main gaseous product, while in the solid phase Fe_3O_4, $FeCl_2$ and C are found. At a 1 : 2 molar ratio (Fig. 2), $FeCl_3$(s) appears in the solid phase below 600 K, while Fe_2Cl_6(g) is the predominant chloride product at higher temperatures. Above 1100 K, $FeCl_2$(g) is the most stable chloride product. Figure 3 illustrates the equilibrium composition in the $FeO + Cl_2$ system at a 2 : 3 molar ratio. In this system FeOCl appears in the solid phase below 600 K, and decomposes with the formation of hematite and Fe_2Cl_6(g).

Chlorination of hematite

The chlorination processes of hematite were characterized by anisothermal TG measurements at 10.1 kPa partial pressures of the reactive gases. The mass loss *vs.* temperature curves are shown in Fig. 4. As the products of the chlorination reactions are volatile, the progress of the reactions can be characterized by the relative mass loss of the samples, and this type of representation will be used for the

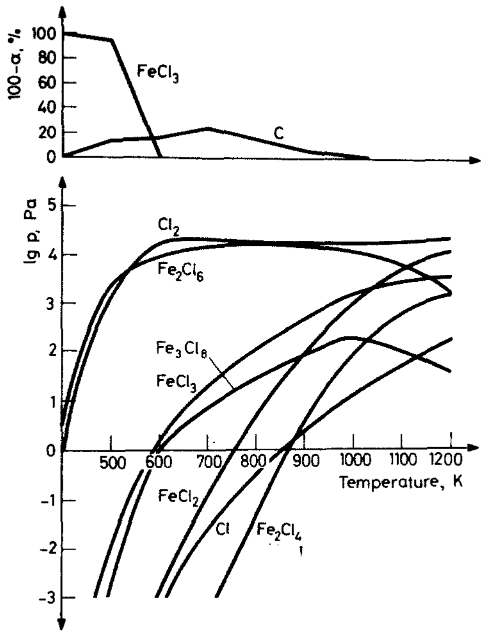

Fig. 1 Equilibrium compositions of the gas and solid phases for the reaction of $FeO+COCl_2$ (molar ratio: 5: 1)

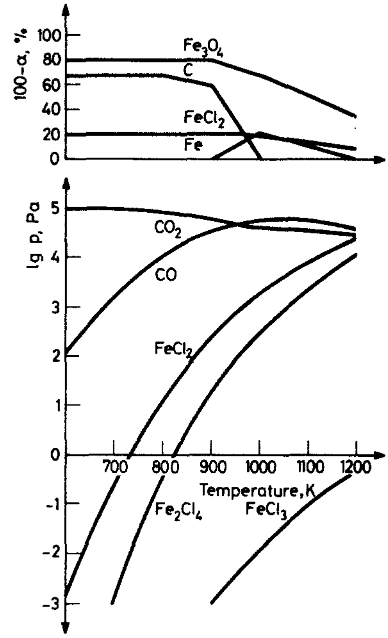

Fig. 2 Equilibrium compositions of the gas and solid phases for the reaction of $FeO+COCl_2$ (molar ratio: 1 : 2)

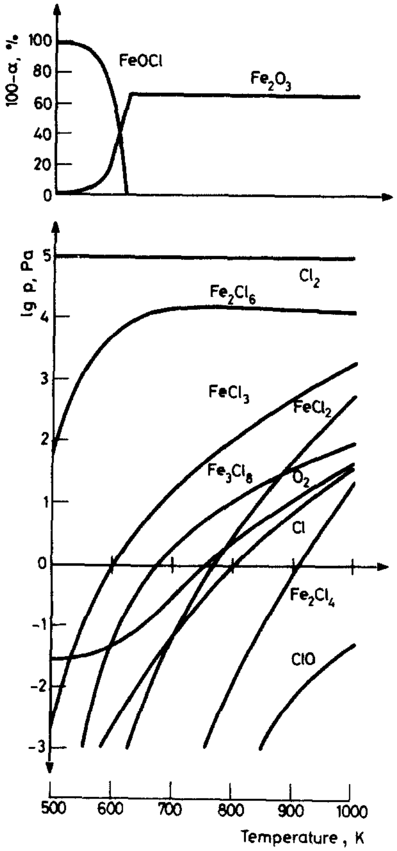

Fig. 3 Equilibrium compositions of the gas and solid phases for the reaction of FeO + Cl_2 (molar ratio: 2: 3)

other systems as well. The starting temperatures of the volatilization processes are 550 K for $COCl_2$, 600 K for CCl_4, 680 K for CO + Cl_2 and 800 K for Cl_2.

The temperature-dependence of the reaction rate (defined as the initial linear slope of the mass loss *vs.* time curves related to unit mass) was studied by means of isothermal TG measurements, as shown in Fio. 5. The shape of the curve is similar to that observed by Neuschütz et al. [1]. In the temperature range where phosgene can exist, the reaction rates for $COCl_2$ are higher than those for CO + Cl_2. At higher temperatures, phosgene begins to decompose, causing a local maximum in the temperature-dependence of the reaction rate. Above 900 K, the data measured with the two chlorinating agents fall on a single curve, indicating the complete decomposition of $COCl_2$. The local maximum at about 900 K for CCl_4 is caused by the thermal decomposition of the chlorinating agent. When the curve for Cl_2 is

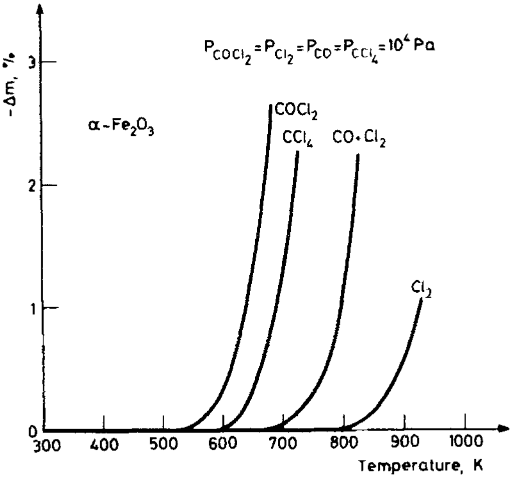

Fig. 4 Mass loss *vs.* temperature curves for the chlorination of hematite. Heating rate 10 deg·min^{-1}, p_i = 10.1 kPa

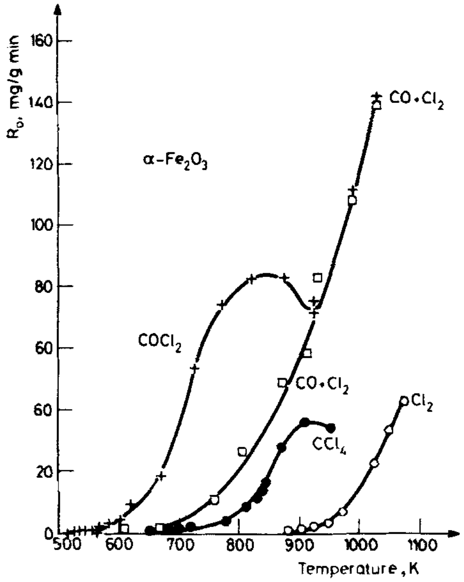

Fig. 5 Temperature dependence of the initial reaction rate for the chlorination of hematite. $p_{COCl_2} = p_{CO} = p_{Cl_2}$ = 10.1 kPa; p_{CCl_4} = 2.1 kPa

compared with that for $CO + Cl_2$, it can be established that in the presence of a reducing agent the reaction starts at much lower (about 200 K) temperatures.

The apparent activation energies derived from the Arrhenius plots are in accordance with the values published in the recent literature, as is shown in Table 1. In the reactions with $COCl_2$ and with Cl_2, lower apparent activation energies were found in the higher temperature ranges, indicating that the reaction rate is influenced by the mass transport.

Table 1 Apparent activation energies (E, kJ/mol) for the chlorination of hematite

Fe_2O_3	Fruehan et al. (1973)	Titi-Manyaka et al. (1972)	Neuschütz et al. (1977)	Present work
Cl_2	167 (1170–1470 K)	96 (970–1170 K)	155 (920–1170 K)	188 (870–1050 K)
			99 (1170–1270 K)	100 (1050–1080 K)
$COCl_2$			61 (720– 820 K)	88 (510– 570 K)
				60 (570– 720 K)
$CO + Cl_2$			102 (870–1170 K)	84 (600– 800 K)
CCl_4				130 (725– 825 K)

Chlorination of wustite

For general characterization of the chlorinating processes, anisothermal TG measurements were carried out. The mass change *vs* temperature curves are shown in Fig. 6. In all cases the reaction starts with considerable mass gain. The curves for the reaction with chlorine (curve 1) and with $CO + Cl_2$ (curve 2) have a very similar character. The chlorination starts with a mass gain at 400 K, followed by two mass loss steps. Above 800 K, the volatilization reaction can be characterized as exponential with T. For CCl_4 and $COCl_2$, the reaction starts only above 470 and 520 K. Two mass gain steps are observed, followed by a rapid mass loss at about 720 and 750 K.

In the system $FeO + Cl_2$, the mass gain (Fig. 6, curve 1) can be attributed to the formation of $FeCl_3(s)$ and $FeOCl(s)$, as anticipated from the TD calculations (Fig. 3). Consequently, the first mass loss part is caused by the gasification of $FeCl_3(s)$ in the dimeric form $Fe_2Cl_6(g)$, while the second one can be explained by the thermal decomposition of FeOCl. The presence of the solid intermediates was detected in separate TG measurements, and also proved by X-ray diffraction analysis of the samples after chlorination. In Fig. 7 anisothermal measurements are shown, where the active gas flow was changed to nitrogen at a given temperature. As it is seen from curve 1, the second mass loss step, attributed to the decomposition of FeOCl, can

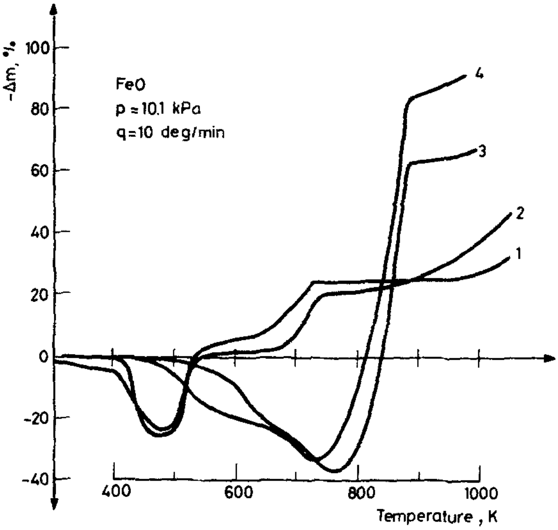

Fig. 6 Mass loss *vs.* temperature curves for the chlorination of wustite. 1: Cl_2, 2: $CO+Cl_2$, 3: $COCl_2$; 4: CCl_4; $p_i = 10.1$ kPa; heating rate: 10 deg·min^{-1}

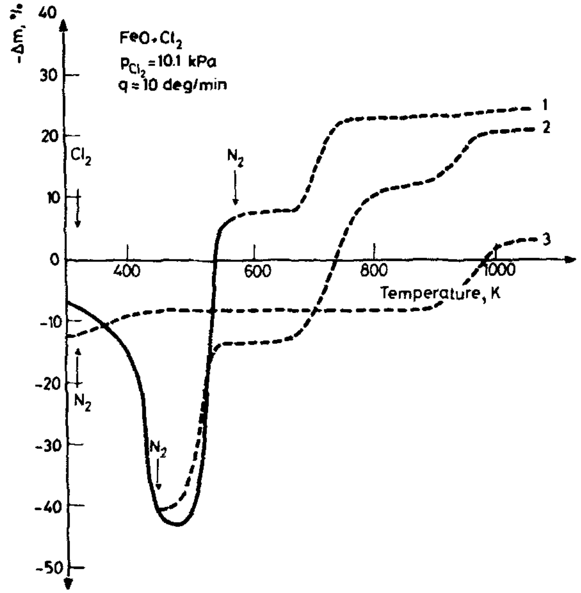

Fig. 7 Mass loss *vs.* temperature curves of wustite. Heating rate: 10 deg·min^{-1}; full line: $p_{Cl_2} = 10.1$ kPa; dotted line in N_2

be observed in the inert atmosphere as well. In the second case (curve 2) the chlorine flow was changed to N_2 at 470 K. During the anisothermal treatment in N_2, three mass loss steps are observed, and are attributed to the sublimation of $FeCl_3(s)$ at 450–520 K, the decomposition of $FeOCl(s)$ at 650–720 K, and the gasification of $FeCl_2$ at 900–970 K. In the third case (curve 3) the chlorine was changed to nitrogen at room temperature. Only $FeCl_2$ was formed in this case, as detected by a simple mass loss step at 950 K. These conclusions based on the TG results were verified by X-ray diffraction analysis of the solid phase after stopping the chlorination reaction at 300, 475, 600 and 720 K, as is seen in Table 2.

Table 2 The composition of the solid phase after the chlorination of wustite

System	Chlorination temperature, K	Products detected by X-ray analysis of the chlorinated samples
$FeO+Cl_2$	300	FeO, $FeCl_2$, Fe_3O_4, α-Fe
	475	$FeCl_3$, $FeCl_2$, $FeOCl$, Fe_2O_3
	600	$FeOCl$, Fe_2O_3
	720	Fe_2O_3
$FeO+Cl_2+CO$	440	$FeCl_3$, $FeOCl$, Fe_3O_4, Fe_2O_3
	570	$FeOCl$, Fe_3O_4, Fe_2O_3
	850	Fe_2O_3
$FeO+COCl_2$	600	$FeCl_2$, Fe_3O_4
	650	$FeCl_2$, Fe_3O_4, Fe_2O_3
	850	Fe_2O_3

In accordance with these results, the $FeO+Cl_2$ system can be characterized by the following overall equations:

$$4\ FeO(s) + Cl_2(g) = FeCl_2(s) + Fe_3O_4(s) \tag{1}$$

$$FeCl_2(s) + 1/2\ Cl_2(g) = FeCl_3(s) \tag{2}$$

$$FeCl_2(s) + Fe_3O_4(s) + Cl_2(g) = FeCl_3(s) + FeOCl(s) + Fe_2O_3(s) \tag{3}$$

$$FeCl_3(s) = 1/2\ Fe_2Cl_6(g) \tag{4}$$

$$FeOCl(s) = 1/3\ Fe_2O_3(s) + 1/6\ Fe_2Cl_6(g) \tag{5}$$

$$Fe_2O_3(s) + 3\ Cl_2(g) = Fe_2Cl_6(g) + 3/2\ O_2(g) \tag{6}$$

$$FeCl_2(s) = 1/2\ Fe_2Cl_4(g) \tag{7}$$

From these observations we can characterize the kinetics of the above phase transformations under isothermal conditions. In Fig. 8 an isothermal TG experiment is shown, where the active gas flow was changed to nitrogen at a given time, and the reaction was followed by anisothermal heating in N_2. The TG curve taken at 480 K starts with a rapid mass gain, followed by slow volatilization. The three mass loss steps observed during the heating in N_2 are attributed to the sublimation of $FeCl_3$(s) (Eq. (4)), the decomposition of FeOCl(s) (Eq. (5)) and the gasification of $FeCl_2$(s) according to Eq. (7). The quantity of solid iron chlorides formed during the reaction can be determined from the mass loss steps, and thus the concentrations of the chloride products and of the unreacted wustite can be calculated.

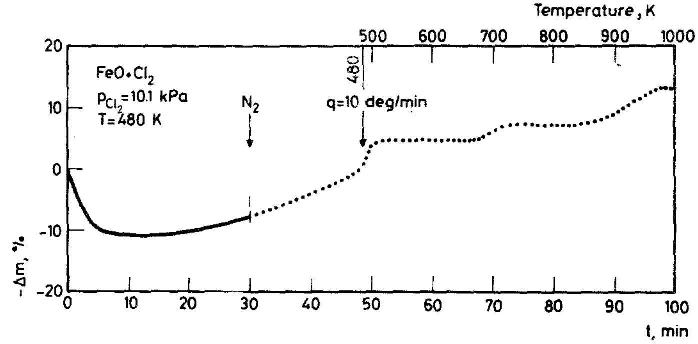

Fig. 8 Isothermal chlorination of FeO followed by isothermal heating in N_2. Full line: $p_{C^1_2}$ = 10.1 kPa, T = 480 K; dotted line in N_2, heating rate: 10 deg·min^{-1}

The chlorination time-dependences of the concentrations of these intermediates and of the uncreated wustite at 480 K are shown in Fig. 9. The total $FeCl_3$ formed during the reaction (including the solid and the gaseous iron trichloride) is represented by curve "$\Sigma FeCl_3$". It is seen that at 480 K the reaction starts with the formation of iron dichloride. Part of the $FeCl_2$(s) is transformed directly to $FeCl_3$(s), while the remaining part reacts with Fe_3O_4(s) and Cl_2(g) according to Eq. (3), when $FeCl_3$(s) and FeOCl(s) are formed. After a maximum value the concentration of iron dichloride decreases with time, due to the consecutive reactions (Eqs (2) and (3)). The end-product, iron trichloride, gradually sublimes during the chlorination.

Similarly as in the FeO + Cl_2 system, the reaction of FeO with CO + Cl_2 (Fig. 6, curve 2) starts at low temperatures with the formation of $FeCl_2$(s), $FeCl_3$(s) and FeOCl(s). These intermediates were detected by X-ray diffraction as well (Table 2). It can be seen from the anisothermal TG curve (Fig. 6, curve 2) that CO plays an

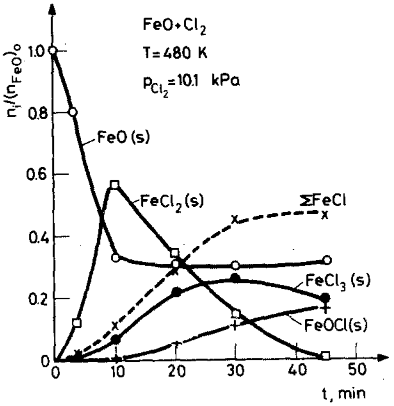

Fig. 9 Time dependence of the concentration of the solid chloride products and of the unreacted wustite during the reacttion of $FeO+Cl_2$ at 480 K

important role in the chlorination process only above 850 K, when the hematite formed starts to react with Cl_2 through the participation of CO.

Figure 10 shows the concentrations of the chloride products and of the unreacted wustite during chlorination with $CO+Cl_2$ at 480 K. The curves display a similar trend as in chlorination with Cl_2. From these curves we can construct the following picture: a layer of $FeCl_2$(s), and later of $FeCl_3$(s), is formed around the unreacted core of wustite. Only after the sublimation of $FeCl_3$(s) can the reaction proceed further, with eventual complete disappearance of FeO(s).

The reactions in the $FeO+COCl_2$ and $FeO+CCl_4$ systems, shown in Fig. 6, were studied in detail earlier [7, 8]. In both cases, iron dichloride is formed during the

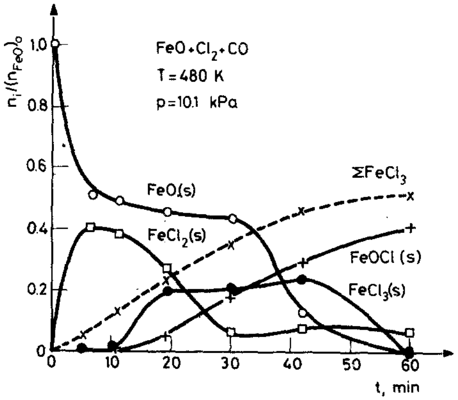

Fig. 10 Time dependence of the chlorination of the solid chloride products and of the unreacted wustite during the reaction of $FeO+Cl_2+CO$ at 480 K

anisothermal chlorination, while the wustite phase is transformed first into magnetite, and at higher temperatures into hematite. The X-ray diffraction analyses of the solid phases are given in Table 2. The reaction with CCl_4 starts at lower temperatures than that with $COCl_2$, and the volatilization also starts at lower temperatures. Thus, CCl_4 seems to be a more reactive agent at these relatively low temperatures.

In order to compare the $FeO+COCl_2$ and the $FeO+CO+Cl_2$ systems, isothermal chlorination experiments were carried out at low and at higher temperatures with $COCl_2$ and with $CO+Cl_2$ (Fig. 11). During the chlorination at 570 K, only a mass gain can be observed with $COCl_2$ (solid iron dichloride and magnetite are formed; see Table 2), while with $CO+Cl_2$ wustite reacts with the Cl_2 via the formation of FeOCl(s), Fe_2O_3(s) and Fe_2Cl_6(g). At higher temperature (860 K), the reaction starts with the formation of $FeCl_2$(s) and Fe_2O_3(s) in both cases, but the mass loss with $COCl_2$ is higher than that with $CO+Cl_2$, due to the difference in the rates of chlorination of the Fe_2O_3(s) formed.

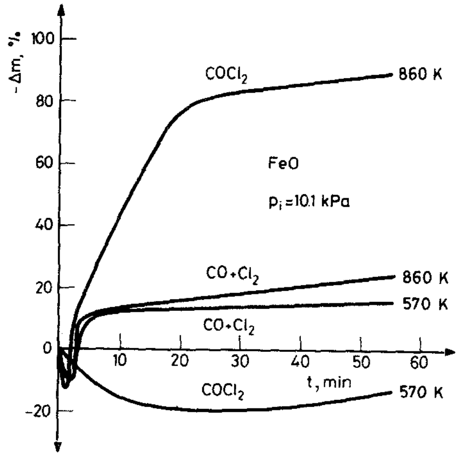

Fig. 11 Mass loss *vs.* time curves for the chlorination of FeO by $COCl_2$ and $CO+Cl_2 \cdot p_i = 10.1$ kPa

Conclusions

Markedly different reactivity sequences were observed in the chlorinations of hematite and of wustite with various chlorinating agents. During the chlorination of hematite, the highest volatilization rate was obtained with $COCl_2$, Cl_2 proving a less reactive chlorinating species. Wustite, however, reacts with chlorine even at moderate temperatures. During chlorination at 480 K, a solid layer of iron dichloride and iron trichloride is formed around the unreacted core of wustite. CO has only a minor effect on the reaction rate at this temperature. With $COCl_2$ and CCl_4, the reaction proceeds via the formation of iron dichloride and hematite. CCl_4 proved to be the more reactive of the two reagents at moderate temperatures. At higher temperatures, the formation of the intermediate chloride products and the transformation of the wustite to hematite become very fast. After the first transition period, therefore, the chlorination rate is determined by the volatilization of the hematite formed during the reactions.

References

1 D. Neuschütz, E. Mann and O. Knacke, Erzmetall, 30 (1977) 464.

2 R. Titi-Manyaka and I. Iwasaki, Trans., AIME, 252 (1972) 307.

3 R. J. Fruehan and L. J. Martonik, Met. Trans., 4 (1973) 2793.

4 G. Daradimos and U. Kuxmann, Erzmetall, 24 (1971) 163.

5 L. Szabó, I. Vassányi and S. Szabó, Sprechsaal, 114 (1981) 437.

6 V. I. Evdokimov, I. Z. Babievskaya, N. F. Drobot, I. Bertóti, I. S. Pap and T. Székely, Zh. Neorg. Khim., 30 (1985) 1507.

7 I. Bertóti, I. S. Pap, T. Székely, I. Z. Babievskaya and L. Bottyán, Thermochim. Acta, 85 (1985) 87.

8 I. S. Pap, I. Bertóti, T. Székely, I. Z. Babievskaya and L. Bottyán, Thermochim. Acta, 92 (1985) 587.

9 I. Bertóti, A. Tóth, I. S. Pap and T. Székely, Therm. Anal., ICTA 80, Birkhäuser Verlag, Basel, Boston, Stuttgart, 1980, Vol. 2, p. 235.

10 I. Barin and O. Knacke, Thermochemical Properties of Inorganic Substances, Berlin, Heidelberg, New York, Düsseldorf, 1973.

Zusammenfassung — Die Reaktionen von Hämatit und Wustit mit Cl_2, $COCl_2$, $CO+Cl_2$ and gasförmigen CCl_4 wurden thermogravimetrisch und röntgendiffraktometrisch untersucht. Thermodynamische Berechnungen wurden mit Computern ausgeführt. Bei der Chlorierung von Hämatit entstehen nur gasförmige Reaktionsprodukte. Die scheinbaren Aktivierungsenergien wurden aus isothermen TG-Kurven berechnet. Bei der Chlorierung von Wustit wird eine Reihe von festen Chloriden gebildet. $FeCl_2(s)$, $FeCl_3(s)$ und $FeOCl(s)$ treten bei der Chlorierung mit Cl_2 oder Cl_2+CO als intermediäre Produkte auf, während bei Reaktionen mit $COCl_2$ oder CCl_4 nur $FeCl_2(s)$ nachgewiesen wurde. Die verschiedenen Chlorierungsmittel wurden hinsichtlich ihrer Wirksamkeit miteinander verglichen und in einer entsprechenden Reihenfolge eingeordnet.

Резюме — Реакции гематита и вустита с Cl_2, $COCl_2$, $CO+Cl_2$ и газообразным CCl_4 были изучены с помощью термогравиметрии, рентгеноструктурного анализа и термодинамических расчетов, проведенных с ЭВМ. При хлорировании гематита образуются только газообразные продукты. На основе кривых изотермической ТГ были вычислены кажущиеся энергии активации. Хлорирование вустита включает образование и превращение ряда твердых продуктов. При взаимодействии с Cl_2 или Cl_2+CO были идентифицированы такие промежуточные продукты, как $FeCl_2$, $FeCl_3$ и FeOCl, тогда как в реакции с $COCl_2$ или CCl_4 — только один $FeCl_2$. Сопоставлены реакции хлорирования различными агентами окислов железа и установлены различия в их реакционной способности.